Influence of ENSO on stratospheric sulfur dioxide injection in the CESM2 ARISE-SAI-1.5 simulations

Chenrui Diao[1], Elizabeth A. Barnes[1], and James Wilson Hurrell[1]

[1]Colorado State University

June 23, 2023

Abstract

Climate and Earth system models are important tools to assess the benefits and risks of stratospheric aerosol injection (SAI) relative to those associated with anthropogenic climate change. A "controller" algorithm has been used to specify injection amounts of sulfur dioxide in SAI experiments performed with the Community Earth System Model (CESM). The experiments are designed to maintain specific temperature targets, such as limiting global mean temperature to 1.5ºC above the pre-industrial level. However, the influence of natural climate variability on the injection amount has not been extensively documented. Our study reveals that more than 70% of the year-to-year variation in the total injection amount (excluding the long-term trend) in CESM SAI experiments is attributed to the El Niño-Southern Oscillation (ENSO). A simplified statistical model further suggests that the intrinsic, lagged response of the controller to the climate can increase the variance of global mean temperature in the model simulations.

Influence of ENSO on stratospheric sulfur dioxide injection in the CESM2 ARISE-SAI-1.5 simulations

Chenrui Diao[1], Elizabeth A. Barnes[1], and James W. Hurrell[1]

[1]Department of Atmospheric Science, Colorado State University, Fort Collins, CO, USA

Corresponding to: Chenrui Diao (chenrui.diao@colostate.edu)

Key Points:

- The SAI controller applied in the CESM2 ARISE-SAI-1.5 simulation is significantly impacted by ENSO.
- The lagged response of the current SAI controller could lead to an increase in the variance of global mean surface temperature.

Abstract

Climate and Earth system models are important tools to assess the benefits and risks of stratospheric aerosol injection (SAI) relative to those associated with anthropogenic climate change. A "controller" algorithm has been used to specify injection amounts of sulfur dioxide in SAI experiments performed with the Community Earth System Model (CESM). The experiments are designed to maintain specific temperature targets, such as limiting global mean temperature to 1.5ºC above the pre-industrial level. However, the influence of natural climate variability on the injection amount has not been extensively documented. Our study reveals that more than 70% of the year-to-year variation in the total injection amount (excluding the long-term trend) in CESM SAI experiments is attributed to the El Niño-Southern Oscillation (ENSO). A simplified statistical model further suggests that the intrinsic, lagged response of the controller to the climate can increase the variance of global mean temperature in the model simulations.

Plain Language Summary

As global temperatures rise due to increasing greenhouse gas (GHG) emissions, more attention has been given to exploring the feasibility of stratospheric aerosol injection (SAI) as a means of counteracting global warming. Several SAI simulations based on numerical climate models utilize a "controller" algorithm to maintain global temperatures by adjusting aerosol injection amounts on an annual basis. However, our findings reveal a strong influence of El Niño-Southern Oscillation (ENSO) on the "controller" regarding the injection amounts. This unexpected influence goes beyond the original design intent of the controller. Statistical analyses further indicate that the current controller, while successfully preventing global warming, can lead to an increased variance in global mean temperature.

1 Introduction

To mitigate global warming and projected future increases in weather and climate extremes, greenhouse gas emissions must be dramatically reduced (Meinshausen et al., 2009; IPCC, 2021). However, current and planned emission reductions will likely not be sufficient to limit global warming to well under the 2ºC goal of the Paris Agreement. This motivates studies exploring climate intervention (or 'geoengineering') as a possible approach to stabilize or reduce global temperatures and possibly buy more time for emission reductions and the implementation of climate adaptation measures. Stratospheric aerosol injection (SAI) may be one of the most effective climate intervention approaches (e.g., Caldeira et al., 2013; NRC, 2015; Xu et al., 2020; NASEM, 2021). By forming reflective aerosols in the stratosphere through injections of sulfate particles (e.g., sulfur dioxide), SAI aims to reflect a small percentage of incoming solar radiation, thus potentially offsetting greenhouse gas warming and minimizing some of the risks associated with anthropogenic climate change.

Climate model simulations have been used to investigate both the benefits and potential risks of SAI in the context of climate change (e.g., Kravitz et al., 2015; Mills et al., 2017; Richter et al., 2022). MacMartin et al. (2014) introduced an SAI 'controller' algorithm to determine the injection amounts and locations of sulfur dioxide needed each year to reach and maintain prescribed temperature targets, such as the global mean surface temperature (GMST), the hemispheric temperature gradient, and the pole-to-Equator temperature gradient (referred to as T0, T1, and T2, respectively in Kravitz et al. 2017). To achieve this, at the end of each simulated year, the controller calculates and compares the annual-mean values of GMST, T1, and T2 with the respective values from the target climate period. A matrix calculation (based on the climate sensitivity to SAI) is then applied to calculate the amount of sulfate particles needed at different latitudes for the next year to offset the differences in GMST, T1, and T2 between the current year and the target climate.

The National Center for Atmospheric Research (NCAR) recently released a new ensemble of SAI experiments using the Community Earth System Model, version 2 (CESM2; Danabasoglu et al. 2020), which also employed this controller algorithm (Richter et al. 2022). The Assessing Responses and Impacts of Solar climate intervention on the Earth system with Stratospheric Aerosol Injection (ARISE-SAI) results demonstrate the effectiveness of the controller algorithm in maintaining the GMST at 1.5ºC above its pre-industrial value (Fig. S1a). The ensemble-averaged sulfate injection amount in ARISE-SAI-1.5 shows a nearly-linear increase with time, which resembles the increase in greenhouse gas (GHG) concentrations under the moderate Shared Socioeconomic Pathway scenario of SSP2-4.5 scenario (O'Neill et al., 2016) used in the simulations. However, the total injection amounts differ significantly across individual ensemble members (Fig. S1b). This suggests that the controller may be responding not only to the forced warming but also to inter-annual temperature fluctuations driven by model-generated internal variability (thin blue lines in Fig. S1a). The El Niño-Southern Oscillation (ESNO) is one of the most dominant modes of internal variability that influences both global as well as regional climate (Ropelewski & Halpert, 1987; Wang et al., 2017). Thus, it is possible that inter-annual variations in injection amounts are related to the controller's response to ENSO, over and above the injection amounts needed to offset the externally-forced global warming. Such responses might introduce unexpected fluctuations in both the SO_2 injection amount and GMST.

Another issue related to the controller is the ‘lagged response’ intrinsic to the controller algorithm. The injection amount determined by the controller for the following year is based on the current year’s climate. If ENSO influences the controller, the injection amount for the following year will be calculated based on both the forced warming and the ENSO-driven temperature changes from the current year. However, as the phase of ENSO can change quickly, even by the following year (Stein et al., 2010). this may lead to a mismatch between the injection amount and the ENSO-driven temperature variation. Consequently, the injection amounts may not adequately maintain the temperature targets, or they may even exacerbate temperature fluctuations in the following year. This mismatch may thus introduce potential side effects to global and regional climate, particularly during years with quick transitions of ENSO.

Inspired by the two potential issues described above, we focus on two questions in this study: (1) How much does ENSO impact the injection amounts determined by the controller; and (2) to what extent does the lagged response of the controller affect the simulated climate?

2 Data and Methods

2.1 Model simulations

Our analyses are based on ensemble simulations using the Community Earth System Model, version 2, with the Whole Atmosphere Community Climate Model, version 6 (CESM2(WACCM6); Danabasolgu et al., 2020). For studies of climate intervention using SAI, representation of the entire stratosphere, including dynamics and chemistry, is needed to capture the transport of stratospheric aerosols and their interactions with stratospheric constituents such as water ozone and water vapor. Similarly, representing key processes and interactions between multiple Earth system components is important, including coupling between the atmosphere, land, ocean, and sea ice, as well as prognostic aerosols and interactive chemistry.

The ARISE-SAI experiments utilize a moderate emission scenario (SSP2-4.5) and simulate SAI deployment in 2035 with a goal of keeping GMST near 1.5ºC above the pre-industrial level (Richter et al. 2022). A 10-member ensemble of ARISE-SAI is compared to an identical 10-member ensemble experiment without SAI (SSP2-4.5 hereafter). More technical details can be found in Richter et al. 2022. We analyze monthly outputs of near-surface air temperature (SAT) and sea surface temperature (SST).

The controller in ARISE-SAI injects sulfur dioxide (SO_2) into four one-grid boxes (15ºS, 15ºN, 40ºS, and 30ºN at 180º longitude) at an altitude of 21.6 km. In this study, we focus solely on the total SO_2 injection amount, which is calculated by adding the amounts at all four injection locations obtained from the controller log document. To investigate the year-to-year changes in injection amount, we calculate the difference in the total SO_2 injection amount between the following year and the current year (ΔSO_2 hereafter).

2.2 ENSO in the model simulations

As described earlier, year-to-year variations of the total SO_2 injection amount may be related to model-generated internal variability, particularly that driven by ENSO. ENSO is a dominant inter-annual mode of climate variability that strongly impacts global temperature (Cai et al., 2015). Our focus, therefore, is on the potential impact of ENSO on the total injection amount in ARISE-SAI.

We compute and examine the commonly-used Oceanic Niño Index (ONI; NOAA 2019) to represent ENSO in CESM2 simulations. Specifically, a standardized ONI is calculated as the 3-month running mean of SST anomalies over the east-central tropical Pacific (5ºN–5ºS, 170ºW–120ºW). The SST anomalies are relative to a 35-year base period from 2035 to 2069. Ensemble-mean values of SST are subtracted from each simulation realization prior to the calculation in order to remove the SST changes driven by external forcings. In order to be comparable with the total sulfate injection amount, which varies annually, the annual mean of ONI is analyzed.

2.3 Simplified statistical model

The controller algorithm determines the SO_2 injection amount for the coming year based on the annual mean temperatures of the past year. However, the GMST and the meridional gradients in temperature for the coming year could differ significantly from the previous year due to ENSO activity. To investigate how the lagged response of the controller influences the variance of GMST in the simulations, we designed a simplified statistical model (SSM hereafter) based on the GMST from the ARISE-SAI and the SSP2-4.5 simulations.

The SSM simplifies the climate system and considers GMST changes only. The GMST in the SSM is set as follows: $T = T_{GHG} + T\_ENSO$, where T_{GHG} and T_{ENSO} represent the GHG warming and the ENSO-driven GMST changes, respectively. To keep in line with the ARISE-

SAI and SSP2-4.5 experiments, the linear fit of the ensemble-mean GMST from the SSP2-4.5 experiment is applied to represent T_{GHG} (shown as dashed blue line in Fig. S2a).

In climate models and observations, ENSO-driven GMST changes occur over different frequencies, and these may affect the climate impacts introduced by the controller's lagged response. Therefore, to analyze the impacts of the lagged response on GMST variance given a certain ENSO frequency, T_{ENSO} in the SSM is simplified to be an idealized monthly time series with a specified variation frequency: $T_{ENSO} = A * sin(\omega t + \varphi)$, where A (the magnitude of ENSO-driven GMST) is obtained based on the linear regression between ONI and detrended GMST in the SSP2-4.5 simulation. The variation frequency and the initial condition of T_{ENSO} are specified by changing the value of ω and φ, respectively. A sample T_{ENSO} with a 3-year frequency is shown in Fig. S2a.

In response to SAI, the SSM has linear sensitivity to the sulfate injection amount, which is calculated based on the linear regression between the total sulfate injection amount in ARISE-SAI and the difference in GMST between SSP2-4.5 and ARISE-SAI (referred to as the "avoided global warming"; Fig. S2b). We use the same controller algorithm in the SSM as is used in ARISE-SAI. Since the SSM only considers GMST and has no spatial information, T1 and T2 are fixed to the target values so that the controller does not respond to these two criteria. It is worth noting that ENSO activity could also influence the sulfate injection locations by changing T1 and T2. However, since our focus here is only on the total sulfate injection amount (which is dominated by the GMST changes), it is reasonable to ignore these two indices in the SSM for now.

3 Results

3.1 Effects of ENSO on the SO_2 injection amount

In addition to significant long-term warming induced by increases in GHG concentrations, ENSO variations can also strongly influence GMST on interannual timescales. This holds true in the ARISE-SAI simulations. Shown in Fig. 1 is the annual mean time series of ONI, GMST anomalies above the pre-industrial level, as well as ΔSO_2 from all ten ensemble members of ARISE-SAI. The average correlation between ONI and GMST is around 0.71, which reveals that approximately 50% of the year-to-year variability of GMST in ARISE-SAI can be attributed to variations of ENSO.

In addition, ΔSO_2 also shows significant year-to-year variation above the steadily increasing injection amount that is required to counter increasing GHG forcing with time (orange lines in Fig. 1). After the ramp-up period (first five years), when the controller initializes the deployment with a mild increase in injection amounts to required values, the variability of ΔSO_2 is similar to that of GMST and ONI, and this is especially during strong ENSO events. Overall, the correlation between ONI and ΔSO_2 is around 0.53. Since the controller determines the injection amounts based on the annual mean GMST from the preceding year, it is clear that ENSO strongly influences the controller's decision. In particular, compared to the total injection amount (Fig. S1b), the year-to-year variation of ΔSO_2 accounts for about 5% to 10% of the total injection amount in any given year, indicating that the controller's response to ENSO should be large enough to detect even during the later period of ARISE-SAI (when the required injection amount is far greater in order to counter the larger GHG forcing).

Although year-to-year variations of ΔSO_2 are highly correlated with ENSO, some large values of ΔSO_2 are unrelated to ENSO-driven GMST changes (e.g., the first few years in member 10; Fig. 1). Since only about 50% of the GMST variance is linearly associated with ENSO, it is possible that other sources of internal variability may be affecting the variation of ΔSO_2, a topic that is outside of the scope of this paper but is likely worthy of further exploration.

To further investigate inter-annual fluctuations of ΔSO_2, Fig. 2a shows the composite map of surface air temperature (SAT) for times when the standardized ΔSO_2 time series is above 0.5 minus when it is below -0.5. The resulting composite pattern looks remarkably El Niño-like (Cane & Zebiak, 1985). In particular, consistent with the high correlation between ENSO and ΔSO_2 shown in Fig. 1, a strong El Niño (La Niña) event corresponds to a positive (negative) ΔSO_2 , indicating the controller is changing its injection rates to offset the warm or cool anomaly in GMST.

To quantify how much the composite map of ΔSO_2 can be explained by ENSO, a linear regression between ΔSO_2 and ONI was constructed as: $\Delta SO_2 = \beta * ONI + r$, where $\beta * ONI$ is the ENSO-driven ΔSO_2, and the residual (r) represents the non-ENSO driven changes in ΔSO_2. About 72% (with a global pattern correlation between Fig. 2a and 2c of 0.85) of the SAT spatial pattern driven by ΔSO_2 can be explained by the ENSO activity, which again emphasizes that interannual variability of the total sulfate injection in ARISE-SAI are dominated by ENSO, an aspect that yet to be documented.

After removing the linear effects of ENSO, the residual pattern of SAT (Fig. 2d) shows warm anomalies over the middle-to-high latitudes of the Northern Hemisphere as well as over tropical regions outside of the western tropical Pacific, reminiscent of a weak El Nino pattern. This suggests that other modes of internal variability (e.g., the North Atlantic Oscillation or the Pacific Decadal Oscillation) might also be important in affecting year-to-year variations of ΔSO_2.

3.2 Lagged response of the controller and increased GMST variance

At the end of each simulated year, the ARISE-SAI controller calculates the injection amounts needed for the next year based on the preceding year's annual mean temperature indices (GMST, T1, and T2). However, since ENSO can change phases quickly within a single year, the temperature indices, especially GMST (T0), might also change quickly in response to this ENSO variability. In this situation, the previously determined injection amount may not adequately satisfy the injection needs of the coming year, or, it may even exacerbate temperature fluctuations.

The schematic diagram in Fig. 3a shows an idealized case of ENSO quickly transitioning from a warm event in year one to a cold event in year two. By the end of the first year, the controller would detect an ENSO-driven global warming anomaly and increase the injection amount in the second year to offset not only the incremental GHG warming but also the warming driven by El Niño. However, if a cold event (La Niña) occurs naturally in year two, the controller's decision would lead to an even greater global cooling than would have otherwise occurred without the controller. Similarly, in the case of ENSO quickly transitioning from a cold event (La Niña) to a warm event (El Niño), the controller would decrease the injection amount by too much and not adequately offset the GHG warming. It follows from this basic example that the year-to-year variability of GMST might ultimately be larger than expected due to the controller responding to ENSO variability. Fast ENSO transitions are apparent in both the ARISE-SAI simulations (e.g., 2056–2057 in Member 004, and 2051–2052 in Member 005; Fig. 1) and in observations (e.g., 2010-2011; not shown).

To further examine how the controller's response to ENSO affects the variance of GMST, we developed a simplified statistical model based on the ARISE-SAI and SSP2-4.5 simulations, in which the idealized "ENSO" signal has only one specific variation frequency (see Section 2.3). When the variation frequency of ENSO is twice the controller's detection frequency (i.e., two years, shown in Fig. 3b), the controller's decision follows the mechanism described in Fig. 3a and leads to a 34% increase in the variance of GMST. However, this is an extreme case, since ENSO typically varies from two to seven years.

We thus further explore the controller's decisions for different ENSO frequencies (Fig. S3). The results show that the controller algorithm always introduces increased variance in GMST, but the magnitudes of this additional variance depend strongly on the hypothetical ENSO frequency. Specifically, when ENSO varies at relatively high frequencies (e.g., panels a and c in Fig. S3), the GMST variance increases by more than 20%. At lower frequencies (such as seven years in Fig. S3d), the controller can adequately account for most ENSO-induced GMST changes, and it only introduces a small increase in the variance of GMST. In other words, the lagged response of the controller is strongly impacted by the frequency of ENSO variability.

Considering the potential issue introduced by the lagged response of the controller, we further test how the variance of GMST would change if the controller made injection decisions on timescales other than annual. For instance, if the controller changed injection amounts every two years (Fig. 4b), the variance of GMST would significantly increase, and GMST would still slowly increase despite the continuous sulfate injection. More extreme cases occur when the controller injects even less often, such as every five years (Fig. 4c). In this case, the controller fails to offset the GHG warming because the injection amount is always behind the increasing GHG concentrations.

A more intuitive way to prevent introducing spurious variance due to the controller's lagged response would be to detect temperature indices more frequently than once-per-year. Results from the SSM for a controller that changes injection amounts monthly are shown in Fig. 4d. In this case, the variance of GMST is decreased by about 30%, which means the controller mutes part of the ENSO-driven GMST variation. However, muting ENSO-driven GMST variability to such an extent might also introduce unexpected climate impacts both globally and locally.

Comparing the GMST variance between the SSP2-4.5 and ARISE-SAI ensemble simulations (Fig. 5a), it is clear that the averaged GMST variance in ARISE-SAI is greater than that in SSP2-4.5 in both early and late periods (2040–2054 and 2055–2069), consistent with the results from the SSM. Despite largely maintaining the mean values of temperature indices, ARISE-SAI introduces significantly greater GMST variance compared to the climate of the target period (2020–2034 in SSP2-4.5). The SSP2-4.5 simulations show a decrease in the GMST variance because of GHG warming; however, variances across individual simulations exhibit a large spread. Thus, due to the limited ensemble sizes (10 members in both the SSP2-4.5 and ARISE-SAI cases), the variance comparison here contains large uncertainties. The results in Fig 5, therefore, are intriguing but are inconclusive on their own. Additional ensemble members would be required to more confidently state that the lagged response of the controller is driving the differences in GMST variance evident between the SSP2-4.5 and ARISE-SAI simulations.

4 Conclusions and Discussion

The controller algorithm in the ARISE-SAI simulations greatly accomplishes its primary goal; that is, to offset GHG warming by maintaining GMST and meridional temperature gradients at the target values. However, we have shown that the controller is also strongly impacted by ENSO activity, and its lagged response to the temperature targets can introduce a mismatch between injection amounts and ENSO-driven temperature variation, and thus, lead to increases in GMST variance. This is especially true for the case when ENSO varies on similar timescales to the controller's detection frequency (set at one year in the ARISE-SAI simulations). Given these two factors, it may therefore be worthwhile to focus efforts on distinguishing and removing GMST variations driven by ENSO from the algorithm, a topic of ongoing work.

In addition, the residual map of the composite analysis in Fig. 2d suggests that other modes of internal climate variability may also disturb the controller, although with smaller magnitudes than that due to ENSO. Additional analyses involving the hemispheric temperature gradient and the equator-to-pole gradient (T1 and T2) could be beneficial to further understand the controller's behavior in response to such modes.

Lastly, we have focused on the global mean temperature in this study. Additional analysis is warranted to determine whether the controller's response to ENSO introduces detectable regional climate impacts.

Acknowledgments

This work was supported by the Defense Advanced Research Projects Agency (DARPA, grant no. HR00112290071). The views expressed here do not necessarily reflect the positions of the U.S. government. We would like to acknowledge high-performance computing support from Cheyenne (doi:10.5065/D6RX99HX) provided by NCAR's Computational and Information Systems Laboratory (CISL), sponsored by the National Science Foundation.

Open Research

The CESM2-WACCM6-SSP2-4.5 (https://doi.org/10.26024/0cs0-ev98) and CESM2-WACCM6-ARISE-SAI-1.5 (https://doi.org/10.5065/9kcn-9y79) simulations applied in this study are produced and maintained by the National Center for Atmospheric Research (NCAR), both of which are publicly available from: https://www.cesm.ucar.edu/community-projects/arise-sai. All Python codes related to this study are available at https://github.com/C-R-Diao/ARISE_Controller_ENSO. At the time of publication, the codes will be converted to a permanent repository on Zenodo.

References

Ben Kravitz, Douglas G. MacMartin, Michael J. Mills, Jadwiga H. Richter, Simone Tilmes, Jean-Francois Lamarque, Joseph J. Tribbia, Francis Vitt. (2017). First Simulations of Designing Stratospheric Sulfate Aerosol Geoengineering to Meet Multiple Simultaneous Climate Objectives. *Journal of Geophysical Research: Atmospheres*, *122*(23), 2169–2897X.

Cai, W., Santoso, A., Wang, G., Yeh, S.-W., An, S.-I., Cobb, K. M., Collins, M., Guilyardi, E., Jin, F.-F., Kug, J.-S., Lengaigne, M., McPhaden, M. J., Takahashi, K., Timmermann, A., Vecchi, G., Watanabe, M., & Wu, L. (2015). ENSO and greenhouse warming. *Nature Climate Change*, *5*(9), 849–859.

Cane, M. A., & Zebiak, S. E. (1985). A Theory for El Niño and the Southern Oscillation. *Science*, *228*(4703), 1085–1087.

Kravitz, B., Robock, A., Tilmes, S., Boucher, O., English, J. M., Irvine, P. J., Jones, A., Lawrence, M. G., MacCracken, M., Muri, H., Moore, J. C., Niemeier, U., Phipps, S. J., Sillmann, J., Storelvmo, T., Wang, H., & Watanabe, S. (2015). The Geoengineering Model Intercomparison Project Phase 6 (GeoMIP6): simulation design and preliminary results. *Geoscientific Model Development*, *8*(10), 3379–3392.

MacMartin, D. G., Kravitz, B., Keith, D. W., & Jarvis, A. (2014). Dynamics of the coupled human–climate system resulting from closed-loop control of solar geoengineering. *Climate Dynamics*, *43*(1), 243–258.

Meinshausen, M., Meinshausen, N., Hare, W., Raper, S. C. B., Frieler, K., Knutti, R., Frame, D. J., & Allen, M. R. (2009). Greenhouse-gas emission targets for limiting global warming to 2 degrees C. *Nature*, *458*(7242), 1158–1162.

Mills, M. J., Richter, J. H., Tilmes, S., Kravitz, B., MacMartin, D. G., Glanville, A. A., Tribbia, J. J., Lamarque, J.-F., Vitt, F., Schmidt, A., Gettelman, A., Hannay, C., Bacmeister, J. T., & Kinnison, D. E. (2017). Radiative and chemical response to interactive stratospheric sulfate aerosols in fully coupled CESM1(WACCM). *Journal of Geophysical Research*, *122*(23), 13,061–13,078.

National Academies of Sciences, Engineering, and Medicine. (2021). *Reflecting Sunlight: Recommendations for Solar Geoengineering Research and Research Governance*. National Academies Press.

National Oceanic and Atmospheric Administration. (2019). *Cold & Warm Episodes by Season*. https://origin.cpc.ncep.noaa.gov/products/analysis_monitoring/ensostuff/ONI_v5.php

National Research Council. (2015). *Climate Intervention: Reflecting Sunlight to Cool Earth*. National Academies Press.

O'Neill, B. C., Tebaldi, C., van Vuuren, D. P., Eyring, V., Friedlingstein, P., Hurtt, G., Knutti, R., Kriegler, E., Lamarque, J.-F., Lowe, J., Meehl, G. A., Moss, R., Riahi, K., &

Sanderson, B. M. (2016). The Scenario Model Intercomparison Project (ScenarioMIP) for CMIP6. *Geoscientific Model Development*, *9*(9), 3461–3482.

Richter, J. H., Visioni, D., MacMartin, D. G., Bailey, D. A., Rosenbloom, N., Dobbins, B., Lee, W. R., Tye, M., & Lamarque, J.-F. (2022). Assessing Responses and Impacts of Solar climate intervention on the Earth system with stratospheric aerosol injection (ARISE-SAI): protocol and initial results from the first simulations. *Geoscientific Model Development*, *15*(22), 8221–8243.

Ropelewski, C. F., & Halpert, M. S. (1987). Global and Regional Scale Precipitation Patterns Associated with the El Niño/Southern Oscillation. *Monthly Weather Review*, *115*(8), 1606–1626.

Stein, K., Schneider, N., Timmermann, A., & Jin, F.-F. (2010). Seasonal Synchronization of ENSO Events in a Linear Stochastic Model. *Journal of Climate*, *23*(21), 5629–5643.

Tilmes, S., Richter, J. H., Kravitz, B., MacMartin, D. G., Mills, M. J., Simpson, I. R., Glanville, A. S., Fasullo, J. T., Phillips, A. S., Lamarque, J.-F., Tribbia, J., Edwards, J., Mickelson, S., & Ghosh, S. (2018). CESM1(WACCM) Stratospheric Aerosol Geoengineering Large Ensemble Project. *Bulletin of the American Meteorological Society*, *99*(11), 2361–2371.

Wang, C., Deser, C., Yu, J.-Y., DiNezio, P., & Clement, A. (2017). El Niño and Southern Oscillation (ENSO): A Review. In P. W. Glynn, D. P. Manzello, & I. C. Enochs (Eds.), *Coral Reefs of the Eastern Tropical Pacific: Persistence and Loss in a Dynamic Environment* (pp. 85–106). Springer Netherlands.

Xu, Y., Lin, L., Tilmes, S., Dagon, K., Xia, L., Diao, C., Cheng, W., Wang, Z., Simpson, I., & Burnell, L. (2020). Climate engineering to mitigate the projected 21st-century terrestrial drying of the Americas: a direct comparison of carbon capture and sulfur injection. *Earth System Dynamics*, *11*(3), 673–695.

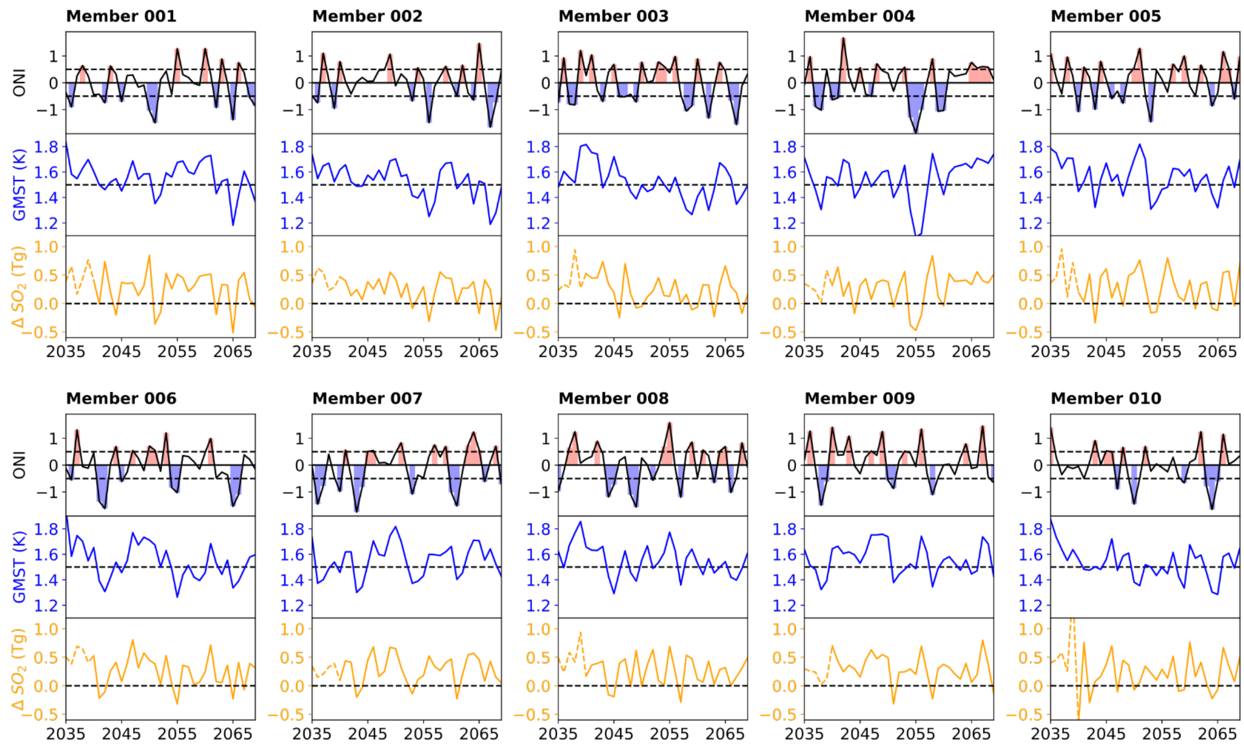

Figure 1. The annual-mean time series of (upper) Oceanic Niño Index (ONI), (middle) GMST anomalies above the pre-industrial level, and (lower) ΔSO_2 for each realization in ARISE-SAI simulation. The annual ONI anomalies are calculated based on the average of monthly ONI; years with ONI anomalies greater than 0.5 ºC (less than -0.5ºC) are marked with red (blue) bars. The first five years (1935–1939, shown as dashed lines in ΔSO_2 panels) are the ramp-up periods according to the controller algorithm.

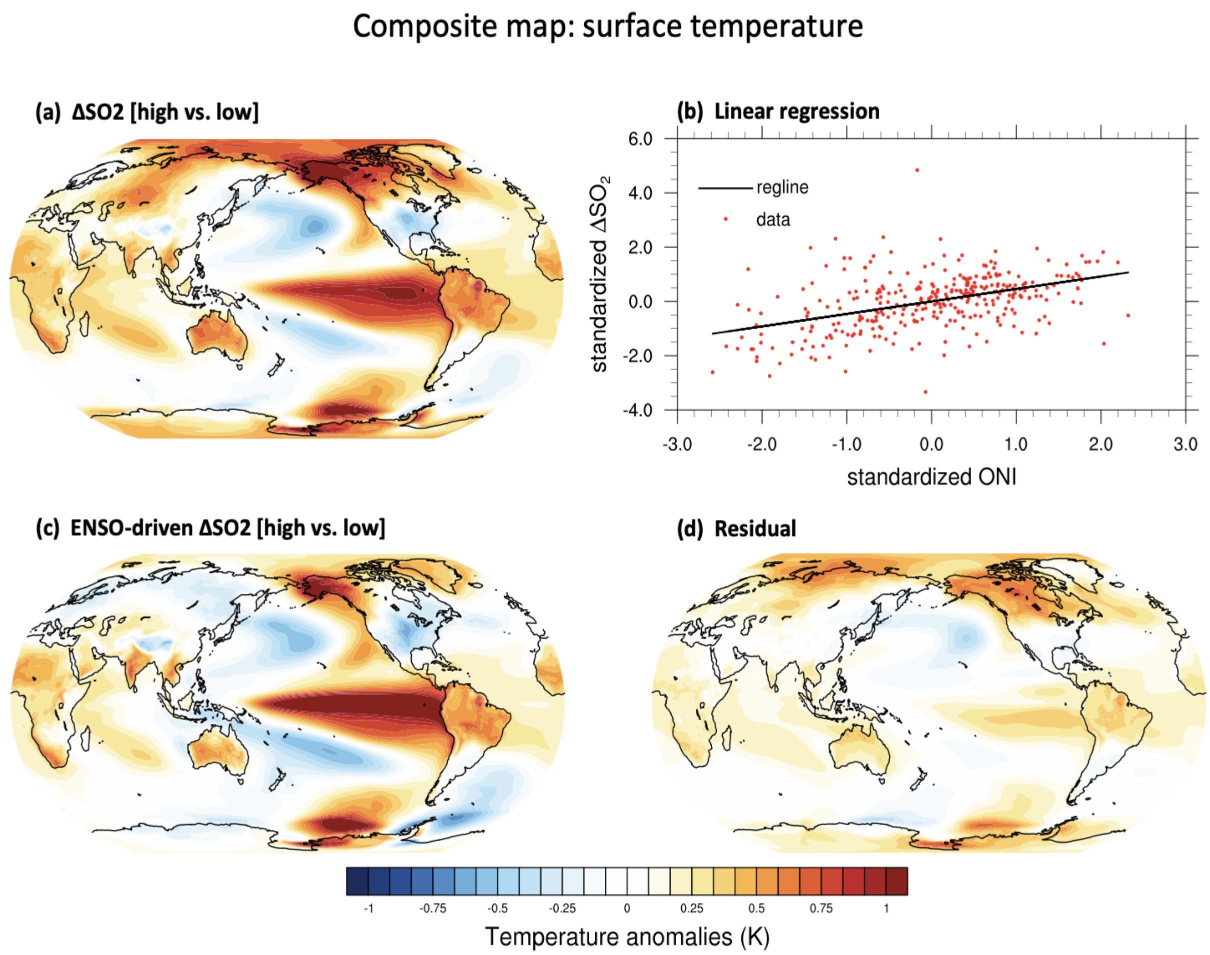

Figure 2. (a) The composite map of surface air temperature (SAT) anomalies in ARISE-SAI when ΔSO_2 (standardized) is greater than 0.5 compared to when ΔSO_2 is less than -0.5. Composite samples are picked from all ensemble members. (b) Linear regression between standardized ONI and ΔSO_2 based on all ten realizations from ARISE-SAI. (c) Same as panel (a) but for ENSO-driven ΔSO_2 calculated from the linear regression in panel (b). (d) The residual map of (a) - (c)

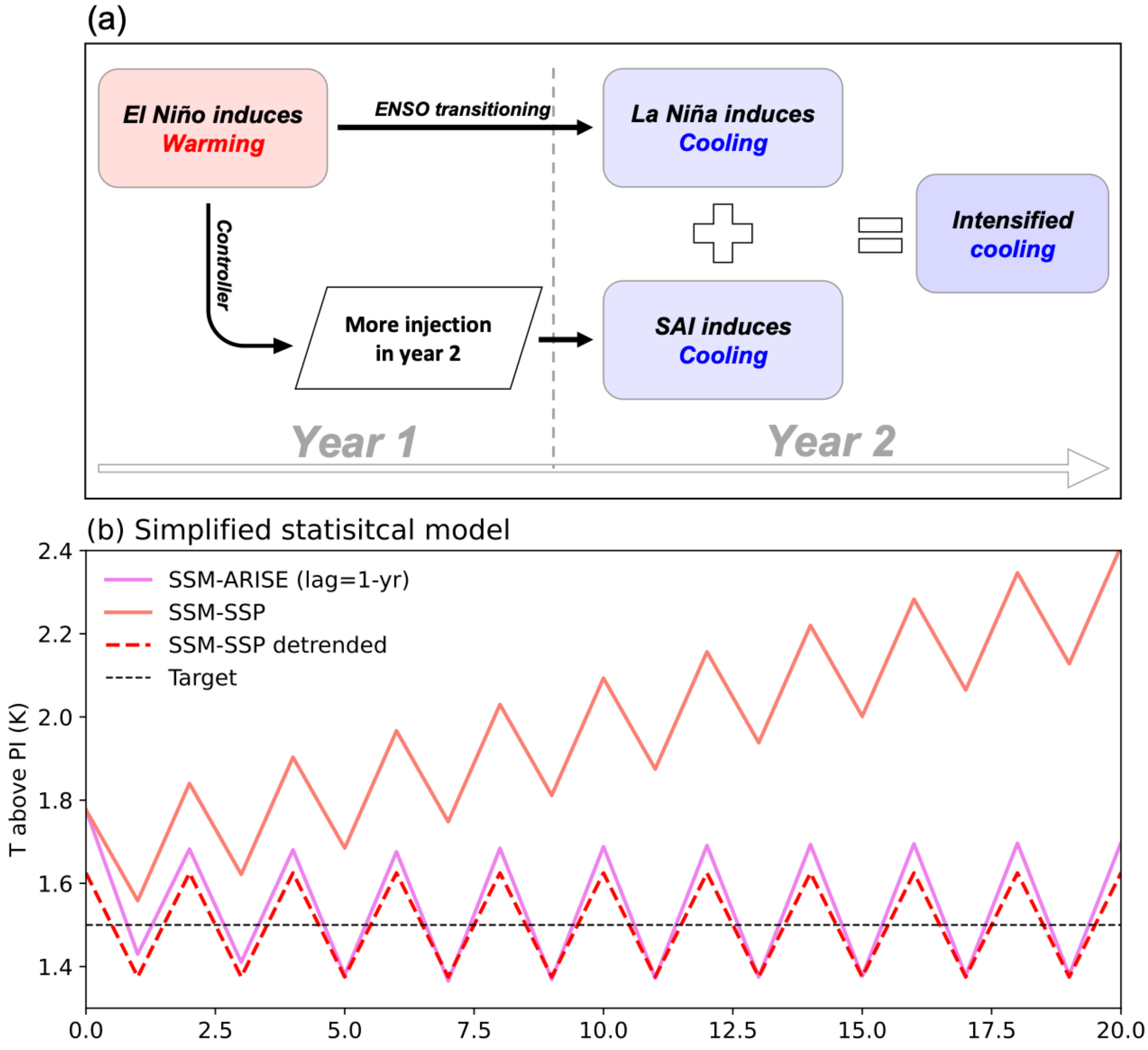

Figure 3. (a) Schematic of intensified cooling during an ENSO quick transitioning case. (b) The results of climate intervention in the simplified statistical model (SSM; see Section 2.3) with idealized "ENSO" at a fixed frequency of 2 years. The red line represents the GMST without climate intervention (SSM-SSP), whereas the blue line represents the GMST with climate intervention (SSM-ARISE). The orange line indicates the detrended GMST without climate intervention (SSM-SSP detrended), which is driven by the idealized ENSO in the SSM. See the Method section for a detailed description of the SSM.

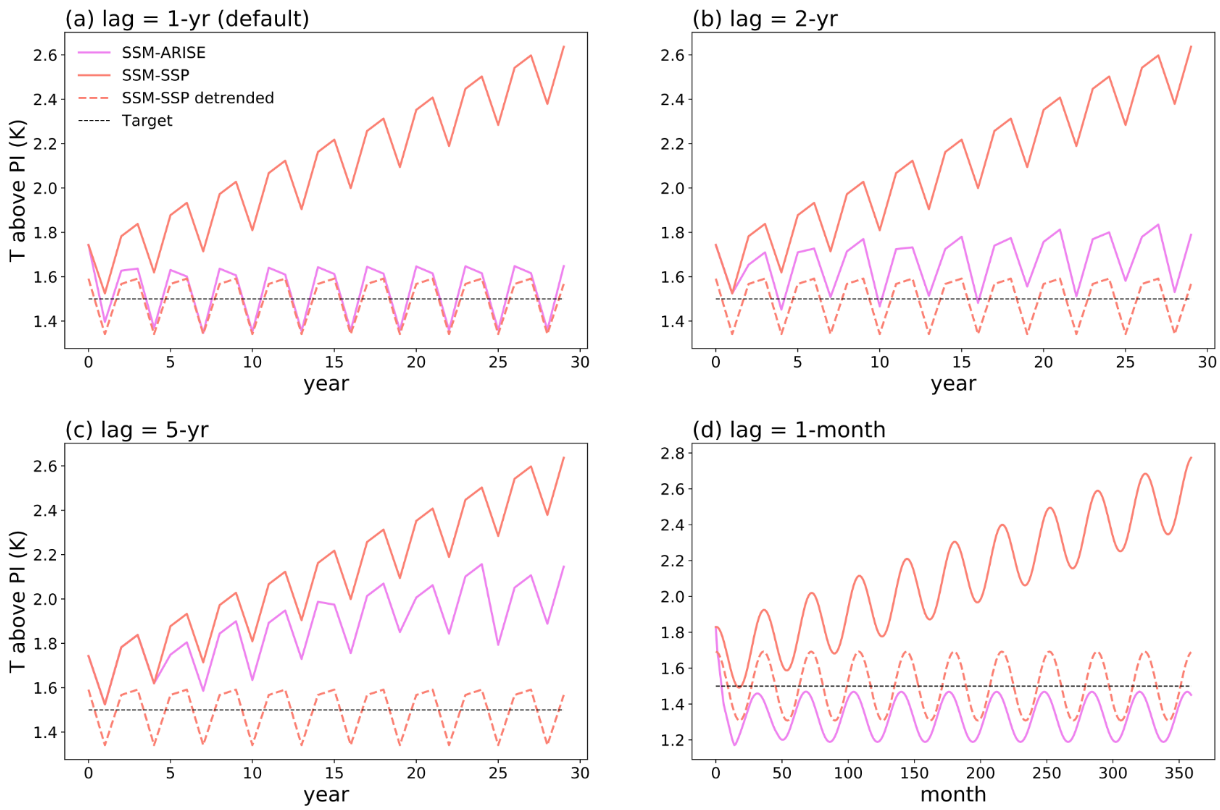

Figure 4. Similar to Fig 4b, but shows the climate intervention results based on the SSM with different controller detection frequencies ranging from 1 month to 5 years. The frequency of the idealized ENSO is fixed at three years in all four cases.

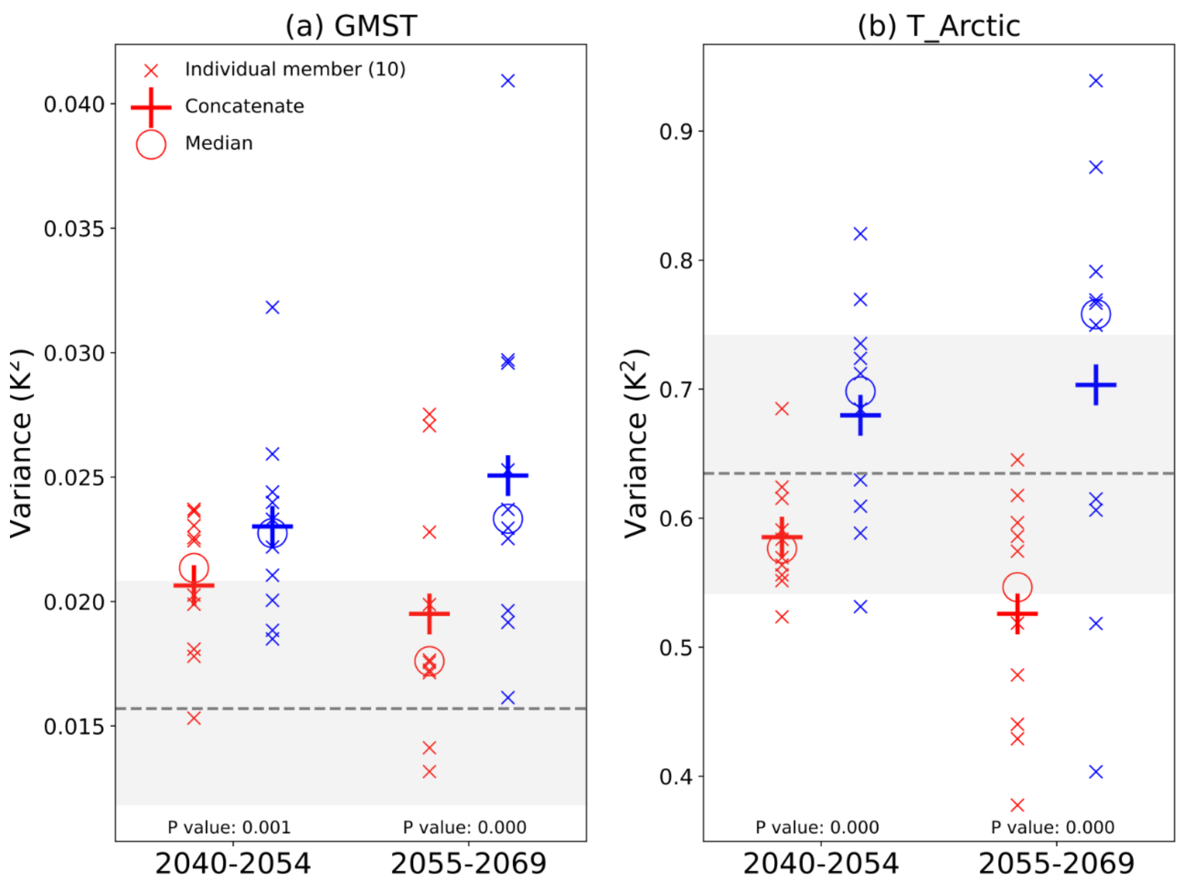

Figure 5. The variance of (a) annual global mean surface temperature (GMST) and (b) the annual Arctic surface temperature (T_Arctic) in SSP2-4.5 (red) and ARISE-SAI (blue) simulations for the period of (left) 2040–2054 and (right) 2055–2069. Cross marks represent the results of each individual ensemble member (10 in each simulation), whereas the circle marks represent the median. The plus marks indicate the variance of concatenated long-term GMST and T_Arctic. The grey shading and dashed line represent the variance spread of GMST for the target period of 2020-2035 from SSP2-4.5 and the variance of concatenated GMST, correspondingly.

Geophysical Research Letters

Supporting Information for

Influence of ENSO on stratospheric sulfur dioxide injection in the CESM2 ARISE-SAI-1.5 simulations

Chenrui Diao[1], Elizabeth A. Barnes[1], and James W. Hurrell[1]

[1]Department of Atmospheric Science, Colorado State University, Fort Collins, CO, USA

Contents of this file

Figures S1 to S3

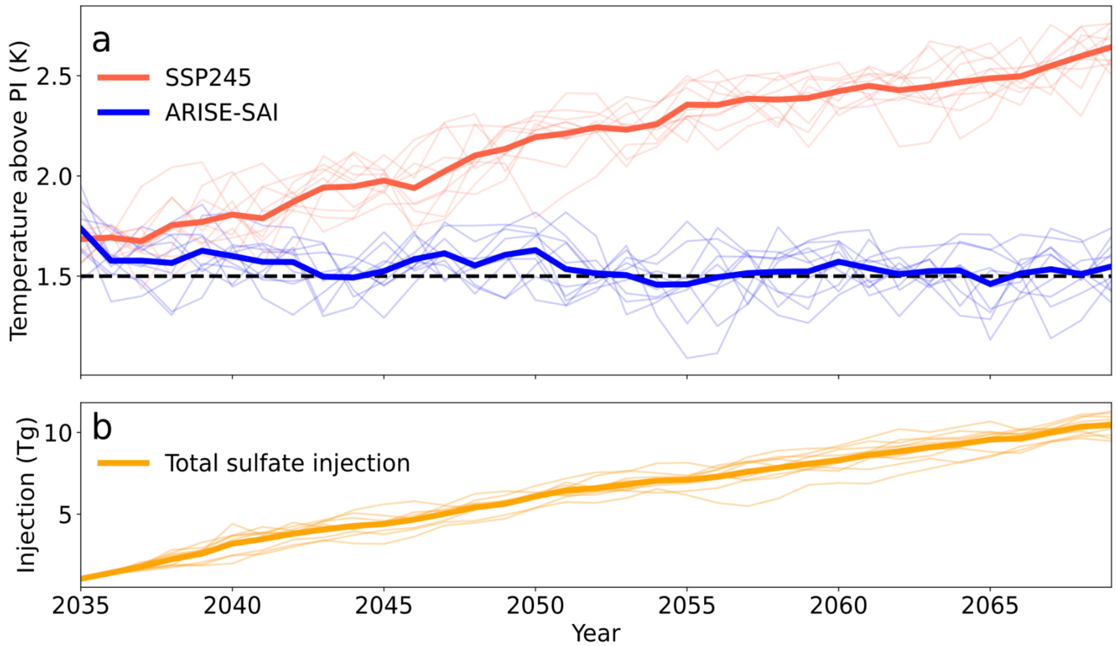

Figure S1. (a) Simulated global mean surface temperature (GMST) above the Pre-industrial (PI) level in SSP2-4.5 (red) and ARISE-SAI (blue) simulations. The thicker lines represent the ensemble-average results, while the thin lines indicate the results from each ensemble member. The black dash line indicates the GMST target (around 1.5 °C above PI level) set in ARISE-SAI runs; (b) The total sulfate injection amount (Tg) in ARISE-SAI simulations. The thicker lines represent the ensemble-average results, while the thin lines indicate the results from each ensemble member.

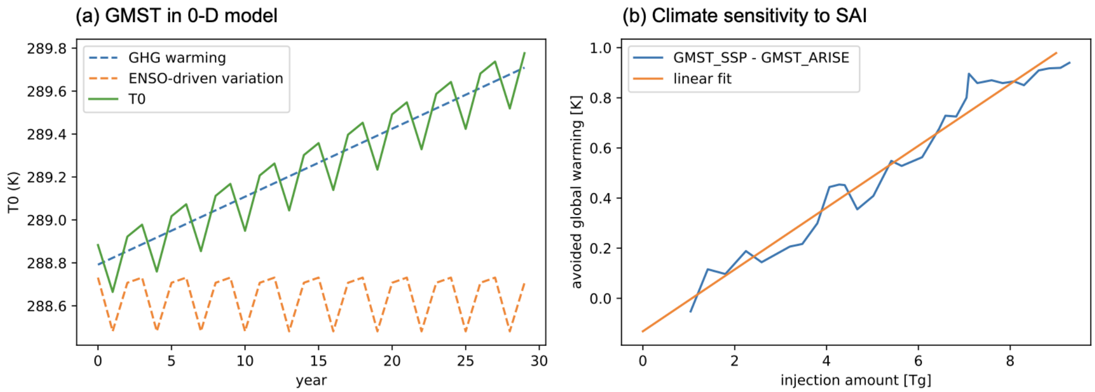

Figure S2. (a) The simplified GMST in SSM. The solid line represents the GMST in the SSM; the straight dashed line represents the GHG warming calculated based on the linear fit of GHG warming in the SSP2-4.5 simulation; the dashed curve represents the simplified ENSO-driven GMST variation; (b) Climate sensitivity to SAI in CESM2(WACCM6) (blue) and the linear fit of the sensitivity (orange) based on the ensemble-averaged result from ARISE-SAI and SSP2-4.5 simulations. The avoided global warming is defined as the difference of GMST between SSP2-4.5 and ARISE-SAI. The linear fit of climate sensitivity is applied in the SSM as its simplified climate sensitivity to SAI.

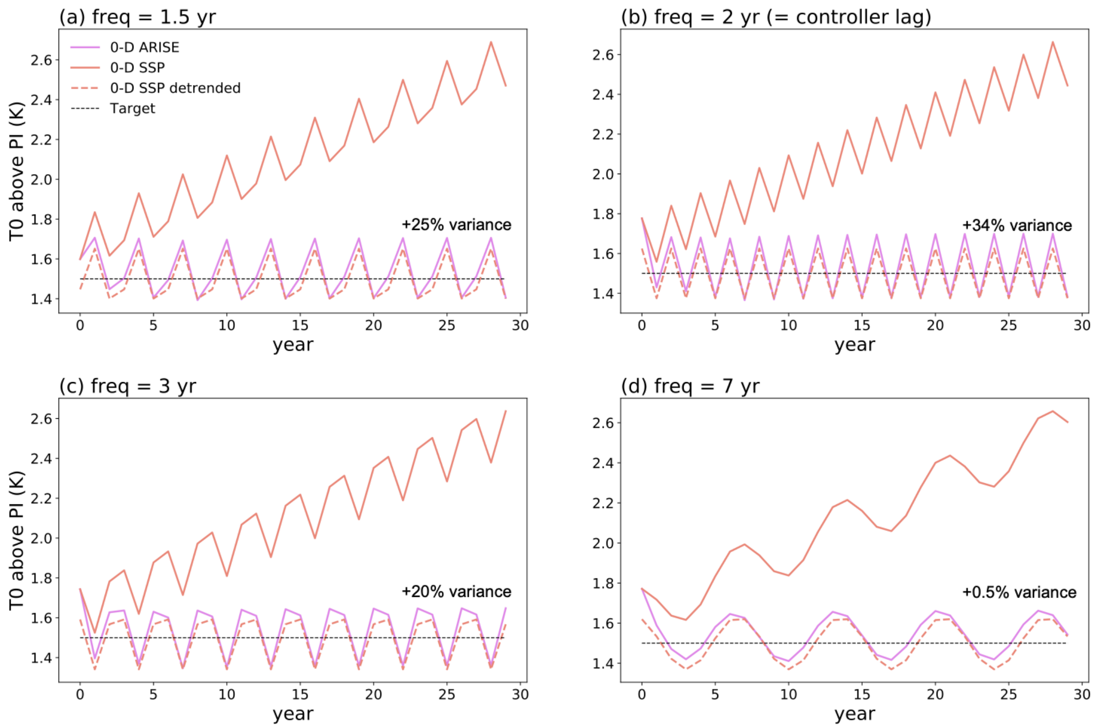

Figure S3. The results of climate intervention in the SSM when the idealized "ENSO" varies at different variation frequencies. The controller's detection frequency is set to the default value (one year). The red line represents the GMST without climate intervention (SSM-SSP), whereas the blue line represents the GMST with climate intervention (SSM-ARISE). The orange line indicates the detrended GMST without climate intervention (SSM-SSP detrended), driven by the idealized ENSO in the SSM.